UCRL-ID-147221

Carbon Nanotube Atomic Force Microscopy for Proteomics and Biological Forensics

A. Noy, J. J. De Yoreo, A. J. Malkin

January 1, 2002

U.S. Department of Energy
Lawrence Livermore National Laboratory

DISCLAIMER

This work was performed under the auspices of the U. S. Department of Energy by the University of California, Lawrence Livermore National Laboratory under Contract No. W-7405-Eng-48.

Lawrence Livermore National Laboratory

Final LDRD Report

Carbon Nanotube Atomic Force Microscopy for Proteomics and Biological Forensics

Principal Investigator:

Aleksandr Noy, CMS, LLNL

Co-Investigators:

James J. De Yoreo, CMS, LLNL

Alexander J. Malkin, UC Irvine

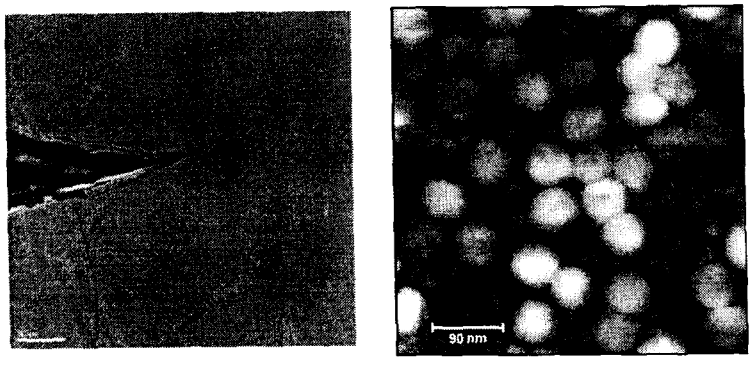

January, 2002

1. Background

The Human Genome Project was focused on mapping the complete genome. Yet, understanding the structure and function of the proteins expressed by the genome is the real end game. But there are approximately 100,000 proteins in the human body and the atomic structure has been determined for less than 1% of them. Given the current rate at which structures are being solved, it will take more than one hundred years to complete this task. The rate-limiting step in protein structure determination is the growth of high-quality single crystals for X-ray diffraction. Synthesis of the protein stock solution as well as X-ray diffraction and analysis can now often be done in a matter of weeks, but developing a recipe for crystallization can take years and, especially in the case of membrane proteins, is often completely unsuccessful. Consequently, techniques that can either help to elucidate the factors controlling macromolecular crystallization, increase the amount of structural information obtained from crystallized macromolecules or eliminate the need for crystallization altogether are of enormous importance. In addition, potential applications for those techniques extend well beyond the challenges of proteomics. The global spread of modern technology has brought with it an increasing threat from biological agents such as viruses. As a result, developing techniques for identifying and understanding the operation of such agents is becoming a major area of forensic research for DOE.

Previous to this project, we have shown that we can use *in situ* atomic force microscopy (AFM) to image the surfaces of growing macromolecular crystals with molecular resolution (*1-5*) In addition to providing unprecedented information about macromolecular nucleation, growth and defect structure, these results allowed us to obtain low-resolution phase information for a number of macromolecules, providing structural information that was not obtainable from X-ray diffraction(*3*). For some virus systems, we have shown that AFM can already resolve some of the gross structural features of the virions themselves even in the absence of crystallization techniques (*5*). Our results show that the limitation on the applicability of this technique to structural studies of viruses and proteins is the size of the AFM tip which currently restricts the lateral resolution to about 10nm at best.

The advent of carbon nanotube AFM probes made it possible to achieve unprecedented resolution in AFM imaging. Because single walled nanotubes have a radius of curvature of about 1nm, their use as AFM tips provides an order of magnitude improvement in lateral resolution! The purpose of this project was to use carbon nanotube tips to develop a new methodology for both determination of macromolecular structures and investigation of macromolecular crystallization. Our intent was to establish this methodology within the LLNL Directorates responsible for proteomics and biological forensics.

2. Fabrication of Carbon Nanotube AFM Probes.

Fabrication of carbon nanotube AFM probes is a challenging task. Not only a 2-nm diameter object (nanotube) has to be manipulated, but also this object has to be placed at the end of 2μm size pyramid (AFM tip). Fortunately, several unique properties of carbon nanotubes help with the task. Besides its geometry the most important feature of a carbon nanotube is its surface energy. The surface energy of a graphitic plane is relatively small, that accounts for many properties of graphite eg, its use as solid lubricant. Yet, the energy changes dramatically when the graphitic plane becomes curved as the carbon nanotube is formed. Smalley and co-workers estimated the cohesion energy of a nanotube wall as a staggering 0.95eV/nm (*6*). This property defines nanotube behavior in interactions with other nanotubes and surfaces. The excess free energy explains the propensity of the nanotubes to form thick bundles (ropes). Also, this surface energy forces nanotubes to adhere to most surfaces even when it requires some bending and a corresponding strain energy punishment. Additional distinct property of nanotubes is their electrical conductivity. Conductivity of single-wall carbon nanotubes is determined by their structure, on average, 1/3 of them is metallic. The conductivity of multi-wall nanotubes is the sum of individual conductivity of its shells and as such most of the multi-wall nanotubes are metallic. The hollow structure of nanotubes is responsible for their phenomenal ability to buckle under load and spring back after the load is released without sustaining any long-term structural damage. All of these properties have significant implications for the task of fabricating the nanotube AFM probes.

2.1 Direct mounting of carbon nanotube bundles onto AFM probes.

We started our fabrication effort in FY2000 by mounting bundles of single-wall carbon nanotubes onto commercial silicon AFM probes. The high-purity nanotube material was generously provided by Prof. C.M. Lieber (Harvard University). Purified bundles of nanotubes typically ranged from 100

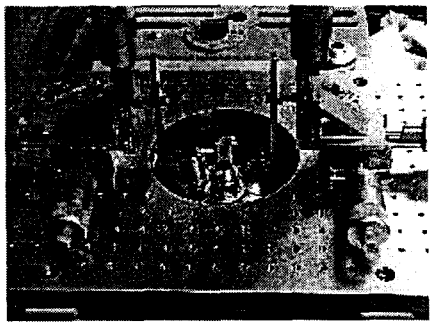

Figure 1. Setup for mounting carbon nanotubes bundles onto AFM probes

to 800 nm in thickness and from 2 to 50 microns in length. The bundles of this size are visible (albeit faintly) in the high-power optical microscope.

To facilitate mounting we constructed a dedicated micromanipulation setup based on a stable inverted optical microscope (Figure 1). Mounting protocol is represented on the Figure 2. Prior to mounting, we dispersed carbon nanotube bundles on the edge of the carbon SEM tape in a way that the bundles were sticking out. We then touched the open region of the tape with an AFM tip to transfer some of the polymer glue onto the tip pyramid. Then we used micromanipulators to maneuver the tip close to the bundle. Then we pulled the bundle out of the SEM tape. In many instances, the bundle will remain stuck to the SEM tape. In these cases we have applied voltage (~10-20V) between the SEEM tape and the AFM tip to burn the bundle in the middle. In 50% of the tries this strategy was successful. Typically the nanotube bundle was still too long and flexible to use it directly as mounted (Figure 3A). We shortened and sharpened the bundle by applying voltage between the AFM tip and the metal surface when the tip was mounted in the scanning probe microscope (we modified our SPM to incorporate

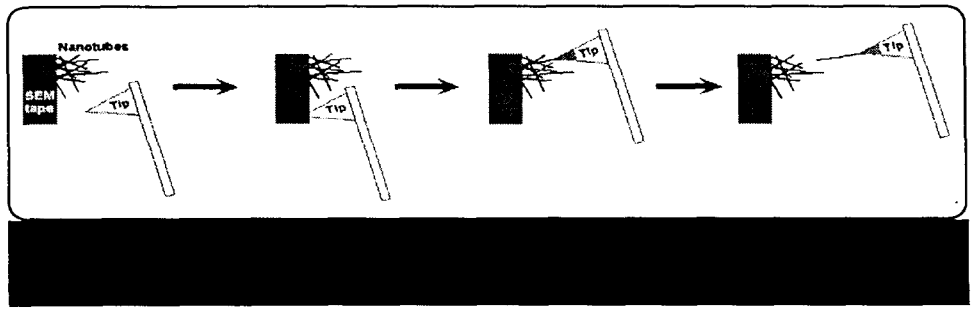

this functionality). An example of the tip after the sharpening procedure is shown on the Figure 3B).

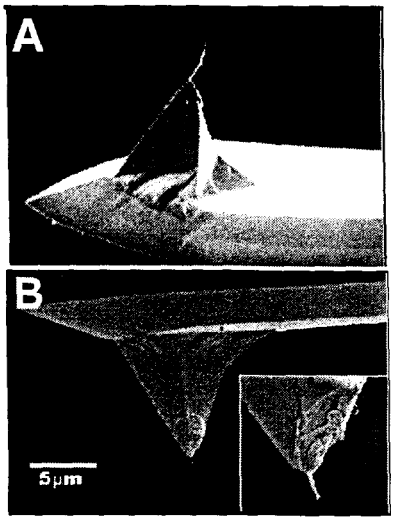

Figure 3. A. Mounted nanotube AFM probe. B. Nanotube AFM probe after sharpening

This method of fabrication has several advantages and disadvantages. It produces robust high aspect ratio AFM probes that resist dulling effectively and have very long lifetime (up to 1 week of continuous imaging). Yet, there are several significant drawbacks;

- Fabrication technique is slow and requires significant manual labor expense.
- There is no possible way for batch fabrication of these probes.
- Even more important, the fabrication process is biased towards large nanotube bundles (they are the ones seen well in the optical microscope!) and as such discriminates against small diameter probes. Yet, these small diameter probes are best for imaging.
- Bundles are very rigid and make poor contact with AFM probe walls. This contact is a critical feature that determined stability of the nanotube probe for fluid imaging. Only a tiny fraction of mounted bundled nanotube probes worked in fluids which made such work impractical.

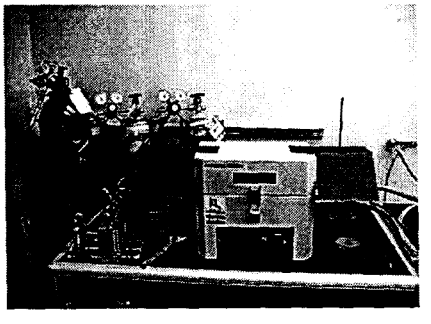

Figure 4. Setup for CVD synthesis of carbon nanotubes

As we saw these drawbacks, we decided to switch our focus to the fabrication of nanotube probes using chemical vapor deposition (CVD) synthesis of carbon nanotubes.

2.2 Fabrication of carbon nanotube AFM probes using chemical vapor deposition. Catalytic CVD production of nanotubes was developed by Smalley

and co-workers (*7*) and later adapted for production of the AFM tips by Lieber and co-workers (*8*). We decided to set up this process to facilitate the production of true single wall nanotube AFM tips, improve the resolution of our images, and enhance the survival of the tips in fluid imaging. In the rest of FY2000 and the beginning of the FY2001 we set up the CVD facility for carbon nanotube synthesis in B154 (Figure 4). Catalytic CVD process relies on the pyrolysis of hydrocarbon gases in presence of catalytic iron nanoparticles (Figure 5). We have also synthesized the catalyst or nanotube synthesis (we are grateful to J. Satcher and R. Reybold (CMS) for help with this synthesis). After that we demonstrated controlled production of single-wall and multi-wall carbon nanotubes (Figure 6) using our setup.

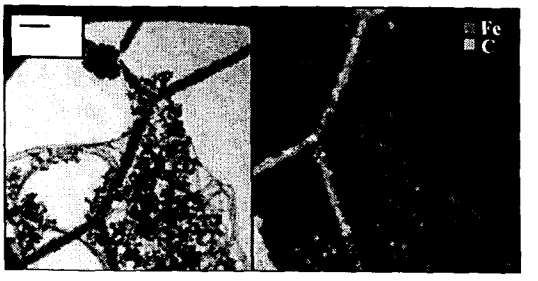

Figure 5. TEM micrograph of carbon nanotubes from the CVD process (left). Elemental map of the same sample area showing Fe nanoparticles that catalyze nanotube synthesis (right). Scale bar corresponds to 100nm

After we established the necessary conditions for reliable nanotube fabrication in our facility we proceeded with fabrication of carbon nanotube probes using our facility. We deposited the catalyst on the AFM tips surface by dipping the tip into the catalyst suspension and ran the probes through the CVD growth cycle. Yet, our initial attempts were unsuccessful. We saw formation of carbon nanotubes on the pyramids of the AFM probes, but none of the nanotubes were emanating out of the end of the tip. To overcome this challenge we had to consider the growth mechanism of these probes. During CVD the nanotubes nucleate randomly on the catalyst particles on the probe surface. There is no preferred growth orientation for them as they grow along that surface. Yet, as the growing nanotube comes to the tip pyramid edge it faces a critical choice. It can bend and continue growing along the surface (i.e. along the pyramid edge) or it can leave the surface and

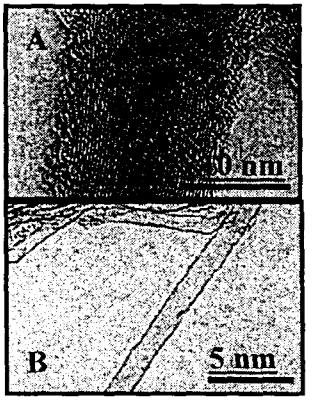

Figure 6. TEM micrographs of multi-wall (A) and single-wall (B) carbon nanotubes.

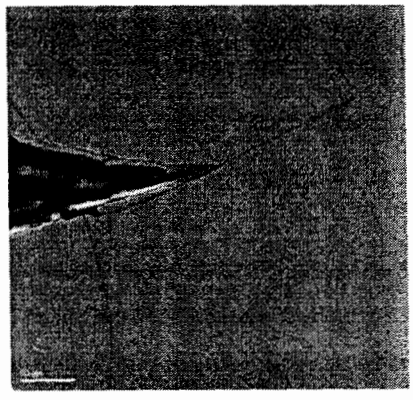

Figure 7. TEM micrograph of a carbon nanotube tip produced by the CVD process

continue growing into the space unsupported. This choice is governed by the balance of the nanotube strain energy and the adhesive energy. If the nanotube chooses to follow the edge, it will be eventually guided to the probe apex where the bend required for it to continue following the surface would be too severe; as the result the nanotube would protrude from the very apex of the pyramid. It turned out that contamination of the pyramid surface greatly reduced the adhesion energy and that shifted energy balance towards the strain energy. As the result, nanotubes were not bending at the probe edges and we could not take advantage of the self-guiding growth mechanism. To solve this problem we had to construct separate oxygen furnace setup dedicated to cleaning the probes. After the cleaning stage was introduced into our tip preparation protocol, we were able to grow usable nanotube AFM tips with >60% yield (Figure 7).

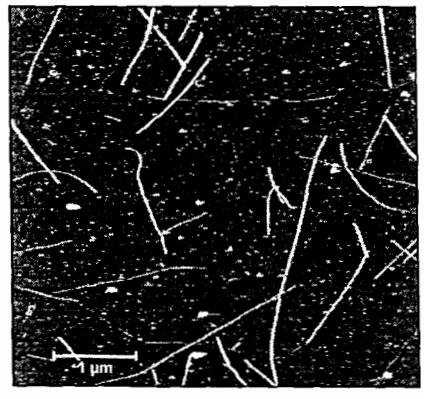

Figure 8. AFM image of a "pick-up" wafer for assembling nanotube tips. Note straight nanotubes, that grew upright (they are pushed down onto the surface by the AFM tip during imaging).

Probe sharpening was another stage in our process that had to be refined as we transitioned to CVD synthesis of nanotubes. As-grown the CVD probes are too long for imaging (i.e. the nanotube is too flexible to sustain scanning); therefore it needs to be shortened with electrical discharge. Yet, the DC pulsing that we used for the mounted nanotube tips was destroying the nanotubes. To achieve efficient shortening we transitioned to using short 50-100µs voltage pulses instead of DC voltages. We built a computerized setup to generate such pulses and tested it on our probes. Using this

technique we were able to fabricate probes that routinely achieved 2-3nm resolution in the AFM images (see imaging results section for examples).

2.3. Direct assembly of carbon nanotube AFM probes.

The CVD process provided us with the effective means to produce nanotube AFM probes. Yet, the majority of the probes consisted of tight nanotube doublets and triplets. As many nanotubes nucleate simultaneously along the probe surface, there is a high probability that more than one of them will be guided to the probe apex. As several of these tubes emerge from the tip apex, they form a tight mini-bundle. Ultimately, this tend ency could be counteracted by reducing the initial catalyst density so that predominately single nanotubes will emerge from the apex, yet that would drive the overall process yield down to unacceptable level. To achieve the fabrication of the ultimate single single-wall nanotube AFM probe we decided to modify our process yet again and to move to direct assembly of the nanotube probes. This assembly process, also pioneered by Lieber and coworkers, uses pre-fabricated wafers of short straight nanotubes grown perpendicular to the support surface (*9*). These wafers are then images by the unmodified AFM probes. As the probe tip glides over an upright nanotube, the nanotube can adhere to the probe sidewall. Since this adhesion energy is very large, the probe tip often "picks up" the nanotube and carries it away from its surface support instead of pushing it down onto the sample. Such "pick-up" probes can then be sharpened using the same protocol as used for the CVD grown probes.

During the rest of the FY2001 we implemented this process in our facility. We used the existing CVD and cleaning setups to fabricate the "pick-up" wafers (Figure 7.) We also successfully assembled a number of probes, sharpened them using our pulse generator (Figure 8) and used them for imaging. Overall, as the result of this project we now have a robust carbon nanotube probe fabrication capability within the CMS Directorate.

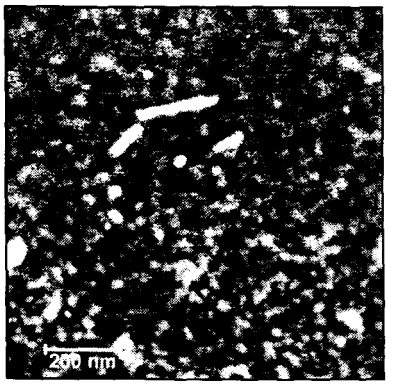

Figure 9. Pieces of a carbon nanotube left on the surface of Nb thin film after sharpening.

3. Biological Imaging using Carbon Nanotube Atomic Force Microscopy

3.1. Resolution comparison: carbon nanotube AFM tips vs. regular AFM tips

Carbon nanotube AFM tips can provide an increase in imaging resolution for several reasons. Obviously small end radii and high aspect ratio geometry contributes to the resolution improvement. Yet, the most important factor is that carbon nanotube has very small adhesive interaction with the sample. These small interactions forces translate into gentler and cleaner imaging. In addition, for a traditional geometry of the AFM tip the adhesion force contribute to an increase in contact area, thus degrading the resolution. Improvements that carbon nanotube AFM offers over the traditional AFM are obvious from a comparison of the test sample (sputtered Nb film) images (Figure 10). These images also demonstrate that CVD nanotube probes are superior to the mounted ones.

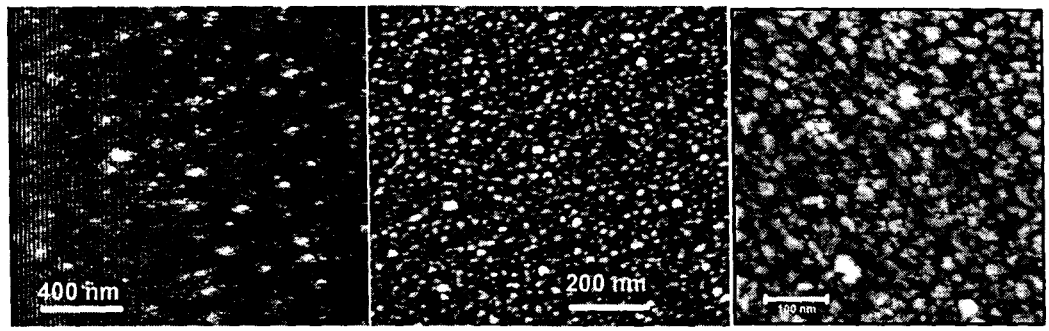

Figure 10. Resolution comparison for different types of AFM probes. (A) Regular AFM tip (B) Mounted carbon nanotube tip and (C) CVD carbon nanotube tip. Note the progressively decreasing scale bars in the images.

3.2 High resolution imaging of viruses.

We have images a number of non-pathogenic plant viruses using our technology. Figure 11 shows an image of a closed-packed layer of the Cucumber Mosaic Virus (CMV). It is clear that use of a carbon nanotube AFM tip allowed us to observe virion substructure. Our observation agreed well with the existing structural model of the outer membrane of this virus showing pentameric and hexameric capsid arrangement. Notably

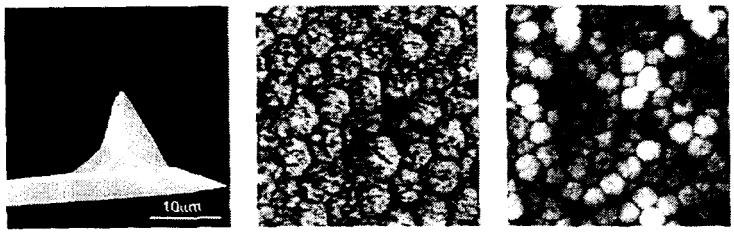

Figure 11 Scanning electron microscopy image of nanotube tip attached to a silicon nitride canteliver tip assembly (A). AFM images in air of CMV adsorbed on mica with a commercial silicon nitride tip (B) and with a nanotube tip (C). In (c) capsomere structure of virions is visible. The image areas are (b) 200x200 nm^2 (c) 290x290 nm^2 .

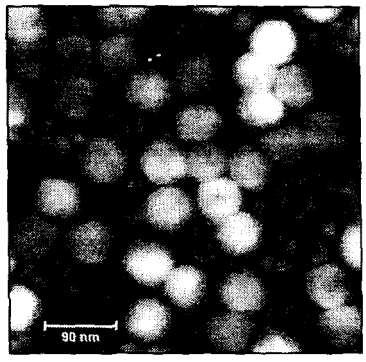

Figure 12. Carbon nanotube AFM image of CMV virions on mica. This image was collected with a CVD-CNT probe.

, neither regular AFM probes nor mounted carbon nanotube probes are able to image isolated viruses on the surface with good resolution (mostly due to mechanical properties of virions). However, we were able to collect reasonable images of single isolated virions using probes produced by CVD techniques (Figure 12). In principle, this type of imaging may be useful for identification of single virions using a database of the virion surface structures.

We have also collected images of a different virus- Turnip Yellow Mosaic Virus (Figure 13).

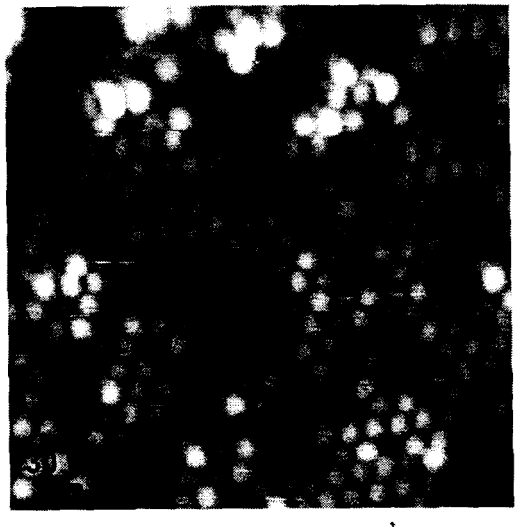

Figure 13. AFM image of TYMV virions on mica

3.3. AFM studies of Chlamedia trachomatis.

We also used our technique to visualize the structural basis of the outer membrane for the bacterium *Chlamedia trachomatis* (COMC). The AFM images revealed that the COMC exhibits a supromolecular structure containing proteins with the size of approximately 50A (Figure. **) This size closely corresponds to the size of the major outer membrane protein (MOMP). The individual molecules in Fig.3b are readily distinguishable and even some sub-molecular details are detectable. We also were

able to image elementary and reticulate bodies of *Chlamedia trachomatis* (Figure 14A).

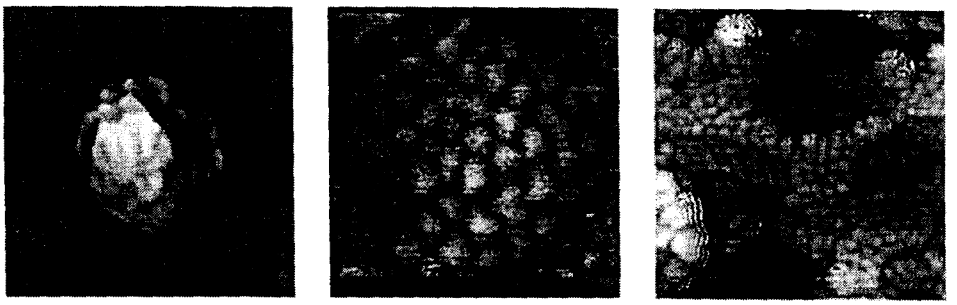

Figure 14. In situ AFM image of (a) Chlamedia trachomatis elementary body, (b) supramolecular structure of COMC, (c) molecular resolution AFM image of COMC in air with a nanotube tip. Images of COMC in air with commercially available AFM tip do not reveal molecular structure. The image areas are 450x450 μm^2, 80x80, 130x130 nm^2 respectively.

3.4 Imaging of DNA-Protein interactions.

We also used our technique to study interactions of proteins with DNA. (Part of this work was also supported by another LDRD project: 01-LW-007). Some imaging examples include first direct visualization of repair protein XPA binding to DNA (Figure ***). In addition, we collected the series of images at different time delays for the interactions of ABF2p DNA packaging protein with plasmid DNA (Figure **). These images provided snapshots of the packaging process that revealed a novel mechanism for the DNA packaging in this system. Based on these images we postulated a mod

el in which protein binding first induces sharp bends in the DNA, which then lead to a collapse of the DNA into a "nucleoid-like" structure.

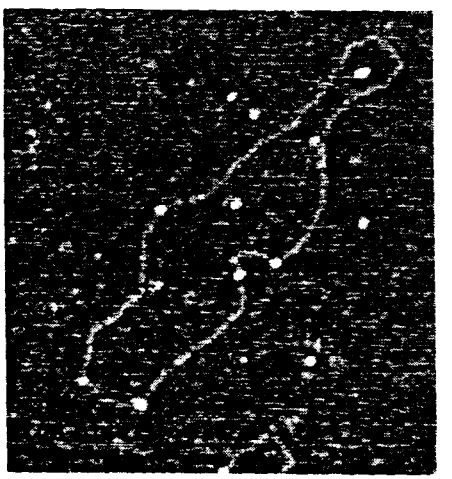

Figure 15. DNA repair protein XPA (white dots) bound to a plasmid DNA molecule.

4.

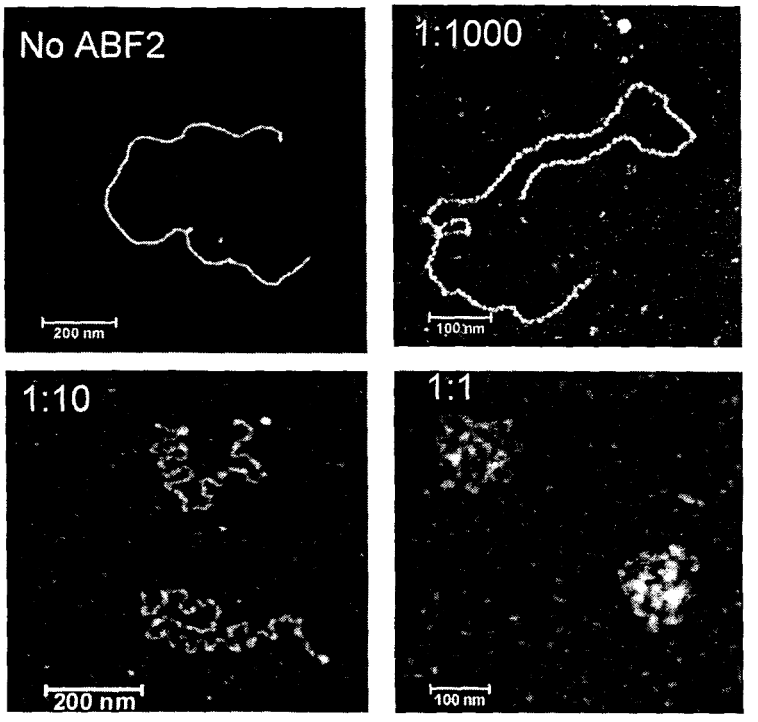

Figure 16. Binding of ABF2p protein to linear DNA molecule as a function of protein concentration. Protein concentration is expressed as protein/DNA base ratio.

Conclusions.. During this project we successfully implemented three different techniques for fabrication of carbon nanotube AFM probes. We demonstrated applications of these probes for imaging different types of biological samples. Successful completion of this project gave CMS and LLNL new expertise in high resolution imaging of biological samples– one of the critical components for the characterization toolkit for biological molecules. In addition, this project created an in-house capability for a sophisticated synthesis of carbon nanotubes, which is already being exploited for other projects.

References:

1. A. J. Malkin, T. A. Land, Y. G. Kuznetsov, A. McPherson, J. J. Deyoreo, *Physical Review Letters* **75**, 2778-2781 (1995).
2. T. A. Land, A. J. Malkin, Y. G. Kuznetsov, A. McPherson, J. J. Deyoreo, *Physical Review Letters* **75**, 2774-2777 (1995).
3. Y. G. Kuznetsov *et al.*, *Biophysical Journal* **72**, 2357-2364 (1997).
4. Y. G. Kuznetsov, A. J. Malkin, A. McPherson, *Journal of Crystal Growth* **196**, 489-502 (1999).
5. A. J. Malkin, Y. G. Kuznetsov, R. W. Lucas, A. McPherson, *Journal of Structural Biology* **127**, 35-43 (1999).
6. M. J. O'Connell *et al.*, *Chemical Physics Letters* **342**, 265-271 (2001).
7. J. H. Hafner *et al.*, *Chemical Physics Letters* **296**, 195-202 (1998).
8. J. H. Hafner, C. L. Cheung, C. M. Lieber, *Nature* **398**, 761-762 (1999).
9. J. H. Hafner, C. L. Cheung, T. H. Oosterkamp, C. M. Lieber, *Journal of Physical Chemistry B* **105**, 743-746 (2001).